


# Characterization of prophages containing “evolved” Dit/Tal modules in the genome of *Lactobacillus casei* BL23

María Eugenia Dieterle<sup>1</sup> · Joaquina Fina Martín<sup>1</sup> · Rosario Durán<sup>2</sup> · Sergio I. Nemirovsky<sup>1</sup> · Carmen Sanchez Rivas<sup>1</sup> · Charles Bowman<sup>3,4</sup> · Daniel Russell<sup>3</sup> · Graham F. Hatfull<sup>3</sup> · Christian Cambillau<sup>5,6</sup> · Mariana Piuri<sup>1</sup> 

Received: 28 April 2016 / Revised: 26 June 2016 / Accepted: 2 July 2016  
© Springer-Verlag Berlin Heidelberg 2016

**Abstract** Lactic acid bacteria (LAB) have many applications in food and industrial fermentations. Prophage induction and generation of new virulent phages is a risk for the dairy industry. We identified three complete prophages (PLE1, PLE2, and PLE3) in the genome of the well-studied probiotic strain *Lactobacillus casei* BL23. All of them have mosaic architectures with homologous sequences to *Streptococcus*, *Lactococcus*, *Lactobacillus*, and *Listeria* phages or strains. Using a combination of quantitative real-time PCR, genomics, and proteomics, we showed that PLE2 and PLE3 can be induced—but with different kinetics—in the presence of mitomycin C, although PLE1 remains as a prophage. A structural analysis of the distal tail (Dit) and tail associated lysin (Tal) baseplate proteins of these prophages and other *L. casei/paracasei* phages and prophages provides evidence that carbohydrate-binding modules (CBM) located within

these “evolved” proteins may replace receptor binding proteins (RBPs) present in other well-studied LAB phages. The detailed study of prophage induction in this prototype strain in combination with characterization of the proteins involved in host recognition will facilitate the design of new strategies for avoiding phage propagation in the dairy industry.

**Keywords** Bacteriophage · *Lactobacillus casei* · Prophage · Baseplate

## Introduction

Bacteriophages infecting lactic acid bacteria (LAB) are an ongoing threat for the dairy industry as they frequently cause milk fermentation failures. Origin of these bacteriophages can be the substrates used for fermentation, surfaces, and aerosol drops, but they are also found as prophages in the bacterial strains used as starters (Durmaz et al. 2008; Garneau and Moineau 2011; Ventura et al. 2006; Verreault et al. 2008).

*Lactococcus lactis* and *Streptococcus thermophilus* are mainly used as starters in the production of dairy products as cheese and yogurt (Ruggirello et al. 2014; Smid et al. 2014). A wealth of studies have been dedicated to the effects of phages infecting these bacteria, as the market of dairy products including probiotic strains in their formulation has notably increased (McFarland 2015). Several strains of *Lactobacillus casei* have purported probiotic properties and are part of commercial formulations (Maldonado Galdeano et al. 2015). The use of these strains is the result of years of research that validated the claimed benefits in food products and led to their approval for human consumption (Douillard et al. 2013a; Douillard et al. 2013b). Noteworthy, phage attack on these specifically chosen strains is particularly deleterious, as they cannot be replaced easily. Accordingly, attention has been

**Electronic supplementary material** The online version of this article (doi:10.1007/s00253-016-7727-x) contains supplementary material, which is available to authorized users.

✉ Mariana Piuri  
mpiuri@qb.fcen.uba.ar

<sup>1</sup> Departamento de Química Biológica, Facultad de Ciencias Exactas y Naturales, Universidad de Buenos Aires, IQUBICEN-CONICET, Buenos Aires, Argentina

<sup>2</sup> Unidad de Bioquímica y Proteómica Analíticas, Institut Pasteur de Montevideo, Montevideo, Uruguay

<sup>3</sup> Department of Biological Sciences and Pittsburgh Bacteriophage Institute, University of Pittsburgh, Pittsburgh, USA

<sup>4</sup> Department of Integrative Structural and Computational Biology, The Scripps Research Institute, La Jolla, CA, USA

<sup>5</sup> Architecture et Fonction des Macromolécules Biologiques, UMR 7257 Centre National de la Recherche Scientifique, Marseille, France

<sup>6</sup> Architecture et Fonction des Macromolécules Biologiques, UMR 7257 Aix-Marseille Université, Marseille, France

focused on the study of phages infecting strains of *Lactobacillus* spp. and particularly of the *L. casei* group (Garcia et al. 2003; Lo et al. 2005; Tuohimaa et al. 2006; Villion and Moineau 2009).

The increasing number of sequenced bacterial genomes has revealed the presence of multiple temperate phages and phage remnants in the genomes of *Lactobacillus* spp. and other LAB (Canchaya et al. 2003; Douillard et al. 2013c). The presence of homologous phage genes spread in different bacterial strains likely suggests horizontal gene transfer between these related species (Baugher et al. 2014).

Previously, we reported the genome sequences of bacteriophages J-1 and PL-1 that infect several *L. casei* and *L. paracasei* strains (Dieterle et al. 2014b). These phages were isolated in the 60s from abnormal fermentations of the Japanese beverage Yakult (Yakult®, Minato-ku, Japan); phage J-1 was isolated first and PL-1 2 years later using a strain resistant to J-1 (Hino 1965; Watanabe et al. 1970). Interestingly, when we analyzed the sequences of phages J-1 and PL-1, we noted that they matched to different regions of the *L. casei* BL23 genome, a widely used laboratory strain very similar to the BD-II, W56, and LC2W commercial probiotic strains (Ai et al. 2011; Chen et al. 2011; Hochwind et al. 2012).

The whole genome sequence of *L. casei* BL23 was reported in 2010 (Maze et al. 2010). A gap between two contigs was identified in the genome at the insertion site of a prophage. Following this, genome pyrosequencing pin pointed two different assemblies corresponding to the integrated and circularized phages. Apparently, only a few cells contained the mobilized prophage since only a single read could be attributed to the phage depleted BL23 genome.

Here, we report the presence of three complete prophages in the *L. casei* BL23 genome that were also present in commercial strains. After exposure to mitomycin C, two of these prophages (PLE2 and PLE3) could be induced, though with different rates. PLE2 and PLE3 genomes were sequenced and their structural proteins were analyzed with special focus in the predicted baseplate proteins, leading to the concept of “evolved” distal tail (Dit) and Tail associated lysin (Tal) (Veesler and Cambillau 2011) bearing carbohydrate-binding modules (CBM) inserted in their sequences. We have also worked out the conditions to study prophage excision and further phage replication by real-time PCR, a useful approach to predict the risk of starter lysis during fermentation processes on other commercial strains of known sequences.

## Materials and methods

### Strain, growth conditions, and prophage induction

*L. casei* BL23 was provided by Dr. Gaspar Perez-Martinez, Instituto de Agroquímica y Tecnología de Alimentos, Valencia,

Spain. A pre-culture of *L. casei* BL23 was grown in MRS medium at 37 °C under static conditions until exponential growth phase and used to inoculate fresh media. When cultures reached an OD<sub>600 nm</sub> 0.1 or 0.2, induction of prophage/s was attempted through the addition of various concentrations of mitomycin C (0.05–0.3 µg/ml) (MC; Sigma-Aldrich Chemical Co., St. Louis, USA). Complete lysis was not observed, but bacterial arrest occurred when 0.1 µg/ml of MC was added to cells at an OD<sub>600 nm</sub> of 0.1. A culture of 500 ml was subjected to the same process, and partial lysates from MC induction were centrifuged to remove remaining bacterial cells and filtered through a 0.45-µm pore size syringe filter. Supernatants were concentrated by ultracentrifugation at 64,000×g for 2 h. Phage pellets were resuspended in phage buffer (20 mM Tris-HCl, 100 mM NaCl, and 10 mM MgSO<sub>4</sub>), and bacteriophage stocks were stored at 4 °C.

Furthermore, a protocol for UV induction described by Raya and H’Bert (2009) was also tested but induction could not be detected.

### Determination of attachment sites

Spontaneous excision of prophages from *L. casei* BL23 chromosome was determined using genomic DNA prepared from an overnight culture grown in MRS medium as described previously (Piuri et al. 2003). DNA sequences were amplified by PCR using *Go Taq* DNA polymerase (Promega, Madison, USA) following the manufacturer’s instructions. Oligonucleotides used to amplify the *attP* site in the circularized form of the phage and the *attB* site after excision from the bacterial chromosome are listed in Table 2. Amplicons were purified and sequenced by MacroGen Corporation, Seoul, Republic of Korea.

### Electron microscopy

Five microliters of concentrated lysates was allowed to sit on freshly glow-discharged 400-mesh carbon-coated Formvar copper grids (Ted Pella Inc., Redding, USA) for 30 s. The grids were then rinsed with distilled water and stained with 1 % uranyl acetate. Virus particles were imaged using a Tecnai Spirit (FEI, Hillsboro, USA) electron microscope operated at 120 kV and a 2000 by 2000 pixel CCD camera.

### Identification of phage proteins

Cesium chloride-purified phage particles were collected by centrifugation at 110,000×g for 45 min. The band was dialyzed in phage buffer (20 mM Tris-HCl, 100 mM NaCl, and 10 mM MgSO<sub>4</sub>) and then centrifugated for 30 min. The pellet was resuspended in 37.5 µl of distilled water, frozen at –70 °C, and then mixed by vortexing. Phage proteins were obtained and analyzed by mass spectrometry as previously described (Dieterle et al. 2014a). Peptides were matched against predicted *L. casei* BL23 proteins.

## Genomic DNA extraction and sequencing

Phage stocks were treated with nuclease (both DNase and RNase), and after enzyme inactivation, phage DNA was phenol extracted as previously described (Durmaz and Klaenhammer 2000). Phage genomic DNAs were sequenced by Ion Torrent (Thermo Fisher Scientific, Waltham, USA), raw reads were assembled using Newbler version 2.1 (454 Life Sciences, Branford, USA), and quality controlled by Consed version 22 (Gordon 2003) at the Pittsburgh Bacteriophage Genome Center. The coverage for *Lactobacillus* phage PLE2 was about 178-fold, and for *Lactobacillus* phage, PLE3 was about 109-fold. The finished sequences were analyzed and annotated in genome editors, including DNAMaster (<http://cobamide2.bio.pitt.edu>), GBrowse (Stein et al. 2002), Glimmer (Delcher et al. 1999), GeneMark (Borodovsky and McIninch 1993), tRNAscan-SE (Lowe and Eddy 1997), and Aragorn (Laslett and Canbäck 2004) and then were manually curated. Each of the determined open reading frames (ORFs) was functionally annotated using BLASTp (Altschul et al. 1990), CDD (Marchler-Bauer and Bryant 2004), and HHpred (Soding et al. 2005).

## Real-time PCR assay for determination of prophage excision

Real-time quantitative PCR was performed using a MyiQ real-time thermal cycler (Bio-Rad, Hercules, USA) with the Real-Mix (Biodynamics, Buenos Aires, Argentina) according to the manufacturer's instructions on the *attB* and *attP* DNA sites of the three complete phages and a chromosomal marker gene (*prtP*). DNA extracted from lysogenic cultures induced with mitomycin C at different times (0, 3, 6, and 9 h) was used as template. The frequency of excision of the prophages was determined by a SYBR Green 1 dye (Life Technologies, Carlsbad, USA) real-time PCR assay. Oligonucleotides were designed using Primer 3 software ([http://genome.wi.mit.edu/genome\\_software/other/primer3.html](http://genome.wi.mit.edu/genome_software/other/primer3.html)), and real-time PCR reactions were performed under the following cycling conditions (5 min at 95 °C, 40 cycles of 20 s at 90 °C, 20 s at 52 °C, and 20 s at 72 °C). Threshold (CT) values were determined by automated threshold analysis with IQTM 5 Optical System Software (Bio-Rad, Hercules, USA). The amplification efficiencies of the templates were determined by serial dilution and calculated as  $E = \exp^{-1/m}$ , where  $E$  is the amplification efficiency and  $m$  is the slope of the dilution curve. Under the conditions of the PCR, the efficiency of the PCR reactions with the various primer pairs was comparable, reaching more than 95 %. PCR assays were performed in triplicate in three separate replicate runs.

CTs were transformed to concentration values with the formula  $\text{Conc} = 10^{((CT - 45.113) / -3.315)}$ , as a derivation of the linear function between CT and the logarithm of the *prtP*

concentration (with an intercept of 45.113 and a slope of  $-3.315$ ;  $R^2 = 0.997$ ). Excision rate was determined as  $\text{attB}/\text{prtP}$  (which can be described as the fraction of bacteria in the culture which suffered excision), while circularization rate was determined as  $\text{attP}/\text{attB}$  (as circular phage concentration is related only to the excised fraction). Means and 95 % confidence intervals were calculated for the excision rate using the R package Rmisc (<http://CRAN.R-project.org/package=Rmisc>), and non-overlapping confidence intervals were considered indicative of significant differences in excision rate.

## Nucleotide sequence accession numbers

PLE2 and PLE3 genome sequences have been deposited in GenBank under accession nos. KU848187 and KU848186, respectively. *L. casei* BL23 accession no. is NC\_010999.1.

## Results

### *L. casei* BL23 carries three complete prophages in its genome

PHAST (Zhou et al. 2011) was used as a prophage predictor to screen for the presence of prophages in the genome of the BL23 strain in combination with a manual procedure to determine the existence of prophage sequences that include the presence of an integrase, portal, terminase, and the tape measure genes.

We were able to identify four prophages. Based on the bacterial genome annotation, three of them (PLE1 to 3) contained all the expected modules (integration and immunity, replication, packaging, virion structure, and lysis) and one of them (PLE4) was probably incomplete, since it was lacking the lysis module. The size and position of the four prophages in the genome of *L. casei* BL23 are shown in Table 1.

While PLE1 and PLE2 are integrated in tRNA genes, PLE3 is integrated in an intergenic region. Interestingly, PLE1 is 99 % identical to the recently sequenced iA2 that was induced from the *L. paracasei* A strain but could not be propagated on any indicator strain (Mercanti et al. 2015). PLE2 and PLE1 (iA2) share 48 % of their DNA sequence. PLE3 is present, as well as PLE2 and PLE1, in commercial probiotic strain genomes such as BDII and W56 but not in the patented probiotic strain LCW2 where PLE1 and PLE2 are also found.

As a preliminary approach, to evaluate if these four prophages could be spontaneously released from the bacterial chromosome, we used the strategy depicted in Fig. 1a. We designed flanking (F flank) primers that only amplify a PCR product if excision had occurred and another set of primers (Circ) that only yield a product if the circularized form of the phage DNA is present. In the latter case, the amplicons should contain the reconstructed *attB* and *attP* sites, respectively. The

**Table 1** Prophages identified in *L. casei* BL23 genome

Name	Position in genome	Size (kb)	Integration site
PLE1	928,670–962,834	34.16	3' ARN <sup>t<sup>leu</sup></sup>
PLE2	1,043,251–1,078,318	35.07	3' ARN <sup>t<sup>arg</sup></sup>
PLE3	1,248,384–1,289,388	41.01	Intergenic region
PLE4 <sup>a</sup>	559,249–602,091	42.84	–

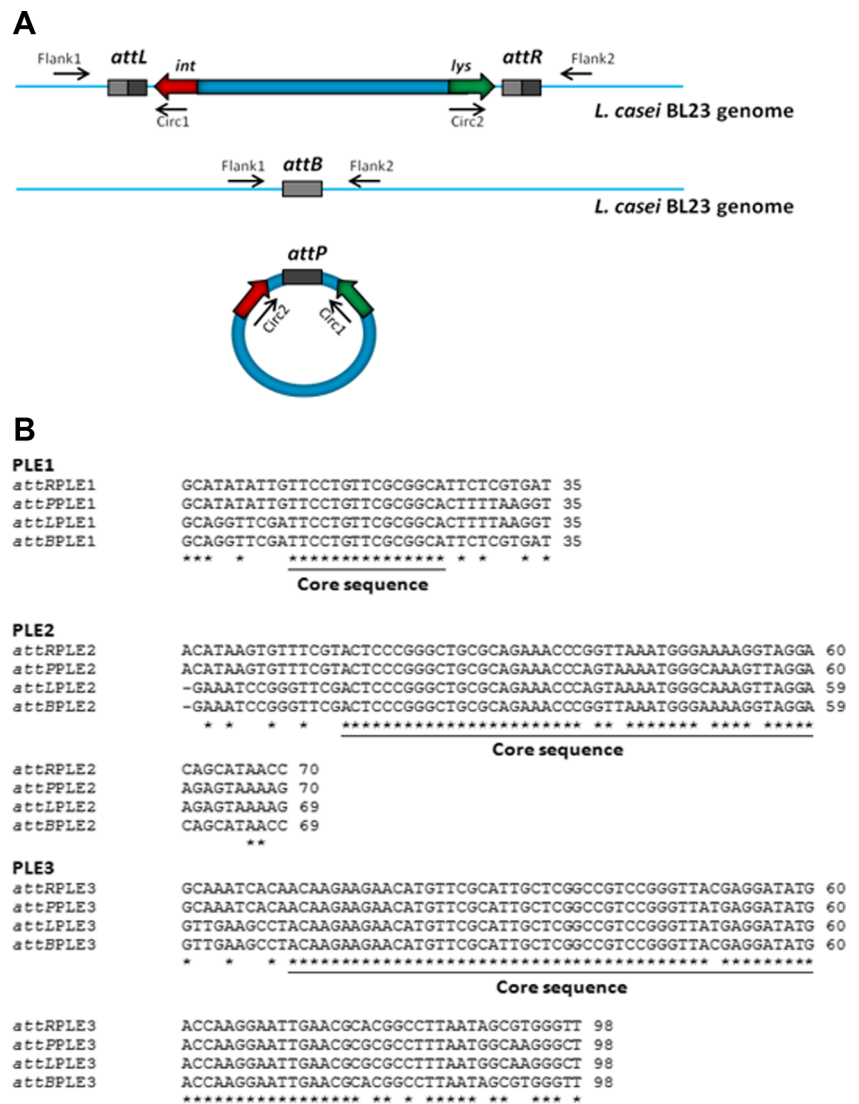
<sup>a</sup> Incomplete phage

*attL* and *attR* sequences were obtained directly from the annotated bacterial genome. Oligonucleotides used in this study are shown in Supplementary Table S1.

Several attempts to obtain a PCR product with primers flanking PLE4 or for detection of the circularized form failed, in agreement with our prediction that PLE4 was an incomplete or remnant prophage.

Alignment of the *attL*, *attR*, *attP*, and *attB* sites for the three complete prophages is shown in Fig. 1b, and the core sequences for each are underlined. For PLE1 and PLE2, phage integration complements the 3' end of the tRNA genes for leucine and arginine, respectively, indicating that integrase-mediated insertion of the prophages leads to the reconstruction of the functional tRNA genes. PLE3 is integrated

**Fig. 1** Excision of PLEs. **a** Schematic representation of the strategy used to evaluate spontaneous excision of PLEs. Flanking primers (*flank1* and *2*) can only amplify a PCR product if excision of the prophage occurred. Circularize primers (*circ1* and *2*) only can amplify a product after excision and circularization of the prophage genome. **b** Clustal alignment of *attR*, *attP*, *attL*, and *attB* of the PLE1, PLE2, and PLE3. The core sequence is underlined



in an intergenic region between LCABL\_12870 and LCABL\_13490.

### Induction of prophages

To test if one or more prophages could be induced from *L. casei* BL23, cultures at early exponential growth phase were exposed to mitomycin C (MC) and OD<sub>600 nm</sub> was monitored over time. Although bacterial lysis was not evident, an arrest of growth was observed for the treated culture (Fig. 2). Aliquots of control and MC-treated cultures were obtained after 0, 3, 6, and 9 h. Cell pellets were used for total DNA extraction, and the supernatant from time point 9 h was filtered and concentrated by ultracentrifugation to recover phage particles (see below).

To evaluate prophage induction/excision, total bacterial genomic DNA from the different time points after treatment with MC was used as template for a real-time quantitative PCR assay on *attP* (present in the circularized prophages) of the three complete prophages (PLE1, 2, and 3) and the correspondent *attBs* (reestablished on the bacterial chromosome after excision) and *prtP* (bacterial chromosomal gene) used as reference of total bacterial DNA. The sequence of the primers used is shown in Table 2. This assay is an adaptation of that described by Lunde et al (2000). To apply this method, first we verified that all the templates used in the comparison for prophage excision had the same amplification efficiencies (see “Material and methods”).

To determine the induction rate of the prophages, the *attB/prtP* ratio was calculated at the different time points (Fig. 3). A spontaneous induction at very low rates (<0.007) in the absence of MC induction was detected for all prophages,

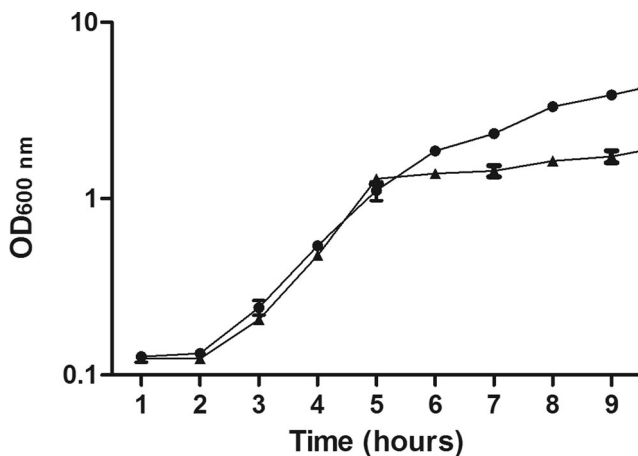


**Fig. 2** Growth curve of *L. casei* BL23 after mitomycin C induction. *L. casei* BL23 cells were grown until an OD<sub>600 nm</sub> of 0.1. The culture was split in two and one half was kept as control (circles) and mitomycin C (0.1 µg/ml) was added to the other half (triangles). OD<sub>600 nm</sub> was monitored over time, and cells were collected at time points 0, 3, 6, and 9 h. The supernatant from the partially lysed culture at time point 9 h was collected for electron microscopy visualization, sequencing, and MS analysis of induced prophages

indicating a very low frequency of the excision event or that excision only occurs in a small bacterial population in this condition. When MC was added, the *attB/prtP* ratio increased for all prophages but it did not remain constant; a peak was observed after 6 h for the three prophages (0.1 for PLE1, 1.1 PLE2, and 0.5 PLE3) corresponding to the exponential growth phase of the strain (Fig. 2). For PLE2, this value was close to 1 suggesting that in the whole bacterial population this prophage was delivered from the bacterial chromosome. At time point 9 h, a decrease was observed consistent with dynamic stages of excision/integration. This pattern has been also observed for phage phiLC3 and was also described for phage lambda where the lysogenic response is favored in stationary phase (Echols 1972; Lunde et al. 2003). Based on these results, only PLE2 and PLE3 were significantly induced after exposure to mitomycin C.

In order to evaluate if these circularized prophages could further replicate to render phage particles, the ratio *attP/attB* at the different time points was calculated for the three prophages. As shown in Fig. 4, this ratio increased over time for PLE2. Since the amount of the *attB* replicon at 6 h is close to that of the chromosomal gene used as control (*prtP*), we hypothesized that the increase in the *attP/attB* ratio reflects DNA replication of the circularized form of PLE2. Moreover, the increase in the calculated ratio approximates an exponential curve (data not shown). But since this technique only allows following the behavior of the whole population, it remains unknown if replication rates differ from cell to cell.

### Genome and structural analysis of PLE2 and PLE3

Filtered and concentrated supernatants of *L. casei* BL23 cultures induced with MC were examined by electron microscopy. Relatively few intact phage particles were visible however, while there were many empty phage heads and disassociated tails (Fig. 5a). The prophage induced has the typical morphology of Siphoviridae, with an isometric head diameter of ~62 nm and a non-contractile tail ~178 nm long (Fig. 5b). No suitable host could be found for the temperate bacteriophage induced using different strains of *Lactobacillus* spp.

CsCl purified partial lysates were used for DNA extraction and further sequencing and subjected to SDS-PAGE for mass spectrometry (MS) analysis of the protein bands. Sequencing data revealed that not only PLE2 but also PLE3 were present in the samples, although the relative coverage was ~13–14 times higher for PLE2 than for PLE3. No DNA from PLE1 was detected confirming the lack of induction of this prophage after mitomycin C induction as shown above.

The predicted genes for PLE2 and PLE3 are listed in Table 2, and the annotated genome maps are shown in Fig. 6. Putative genes could be divided in packaging, structural (head, tail, and baseplate), lysis, immunity, and replication. Analysis of the PLE2 genome revealed 51 potential ORFs and no tRNA

**Table 2** Phages PLE2 and PLE3 predicted genes and gene products

PLE2 gene strand	Start–stop (length-aa)	Best database match with virus (organism, gene)	% aa ident.	Predicted function
1F	57–443 (128)	<i>Lactobacillus</i> phage IA2, 1	99	
2F	446–2176 (576)	<i>Lactobacillus</i> phage IA2, 2	99	Terminase, large subunit
3F	2195–3430 (411)	<i>Lactobacillus</i> phage IA2, 3	99	Portal
4F	3408–4115 (235)	<i>Lactobacillus</i> phage IA2, 4	97	Capsid maturation protease
5F	4120–5349 (409)	<i>Lactobacillus</i> phage IA2, 5	99	Major capsid
6F	5423–5671 (82)	<i>Lactobacillus</i> phage IA2, 6	99	
7F	5685–6011 (108)	<i>Lactobacillus</i> phage IA2, 7	100	
8F	6001–6288 (95)	<i>Lactobacillus</i> phage IA2, 8	99	Head-tail joining
9F	6272–6601 (109)	<i>Lactobacillus</i> phage IA2, 9	99	
10F	6591–6974 (127)	<i>Lactobacillus</i> phage IA2, 10	99	
11F	6986–7633 (215)	<i>Lactobacillus</i> phage IA2, 11	99	Major tail S
12F	6986–7695 (236)	<i>Lactobacillus</i> phage IA2, 11	99 (QC 90))	Major tail L
13F	7710–8075 (121)	<i>Lactobacillus</i> phage IA2, 12	99	Tail assembly chaperone
14F	7710–8313 (202)	<i>Lactobacillus</i> phage IA2, 12	99 (QC 59)	Tail assembly chaperone
15F	8337–11,507 (1056)	<i>Lactobacillus</i> phage IA2, 14	95 (QC 60)	Tape measure
16F	11,514–12,209 (231)	<i>Lactobacillus</i> phage IA2, 15	97	Distal tail
17F	12,206–16,609 (1467)	<i>Lactobacillus</i> phage IA2, 16	89	Tail associated lysozyme
18F	16,587–17,063 (158)	<i>Lactobacillus</i> phage IA2, 17	99	
19F	17,066–17,335 (89)	<i>Lactobacillus</i> phage IA2, 18	97	
20F	17,383–17,769 (128)	<i>Lactobacillus</i> phage J-1, 20	97	
21F	17,750–17,956 (68)	<i>Lactobacillus</i> phage CL1, 23	94 (QC 77)	
22F	17,953–18,414 (153)	<i>Lactobacillus</i> phage CL2, 23	97	Holin
23F	18,416–19,468 (350)	<i>Lactobacillus</i> phage J-1, 23	95	Lysin
24R	21,000–19,849 (383)	<i>Lactobacillus</i> phage J-1, 24	99	Integrase
25R	21,872–21,111 (253)	<i>Lactobacillus</i> phage PL-1, 25	99	
26F	21,891–22,121 (76)	<i>Lactobacillus</i> phage PL-1, 26	100	
27R	23,156–22,377 (259)	<i>Lactobacillus casei</i> BL23, W56, BDII	100	
28R	23,632–23,228 (134)	<i>Lactobacillus</i> phage ilp84, 32	53 (QC 97)	
29R	23,955–23,629 (108)	<i>Enterococcus</i> phage phiFL3A, 3	47 (QC 97)	Trans. regulator/repressor
30F	24,212–24,424 (70)	<i>Lactobacillus casei</i> BL23, W56, BDII	47 (QC 97)	
31F	24,427–25,200 (257)	<i>Brochothrix</i> phage BL3, 34	45 (QC 95)	
32F	25,232–25,555 (107)	<i>Lactobacillus</i> phage A2, 30	38 (QC 72)	Anti-repressor
33F	25,555–25,686 (43)	<i>Lactobacillus casei</i> BL23, W56, BDII	100	
34F	25,700–25,834 (44)	<i>Lactobacillus casei</i> BL23, W56, BDII	100	
35R	26,134–25,823 (103)	<i>Lactobacillus casei</i> BL23, W56, BDII	100	
36F	26,195–26,386 (63)	<i>Lactobacillus</i> phage CL2, 37	60 (QC 75)	
37F	26,400–26,639 (79)	<i>Lactobacillus casei</i> BL23, W56, BDII	100	
38F	26,644–27,138 (164)	<i>Lactobacillus</i> phage Lc-Nu, 28	46 (QC 94)	
39F	27,150–27,380 (76)	<i>Lactobacillus casei</i> BL23, W56, BDII	100	
40F	27,380–28,747 (455)	<i>Lactobacillus</i> phage LfeSau, 36	66	Helicase
41F	28,749 – 29,489 (246)	<i>Lactobacillus</i> phage LfeSau, 37	60	NTP binding domain
42F	29,494–30,001 (169)	<i>Lactobacillus</i> phage LfeSau, 38	40	
43F	30,068–30,865 (265)	<i>Lactobacillus</i> phage phiJB, 21	49	DNA primase
44F	30,855–32,105 (416)	<i>Lactobacillus</i> phage LfeSau, 40	54	Helicase
45F	32,380–32,694 (104)	<i>Lactobacillus</i> phage A2, 40	79 (QC 86)	
46F	32,701–32,985 (94)	<i>Lactobacillus</i> phage IA2, 43	99	
47F	32,972–33,301 (109)	<i>Lactobacillus</i> phage IA2, 44	91	
48F	33,294–33,881 (195)	<i>Lactobacillus</i> phage IA2, 45	90	

**Table 2** (continued)

PLE2 gene strand	Start–stop (length-aa)	Best database match with virus (organism, <i>gene</i> )	% aa ident.	Predicted function
49F	33,868–34,122 (84)	<i>Lactobacillus casei</i> BL23, W56, BDII	100	
50F	34,119–34,523 (134)	<i>Lactobacillus casei</i> BL23, W56, BDII	100	
51F	34,688–35,068 (126)	<i>Lactobacillus</i> phage IA2, 50	96	HNH endonuclease
PLE3 gene strand	Start–stop (length-aa)	Best database match with virus (organism, <i>gene</i> )	% aa ident.	Predicted function
1F	1–573 (190)	<i>Lactobacillus</i> phage ilp84, 1	100	Terminase, small subunit
2F	557–1810 (417)	<i>Lactobacillus</i> phage ilp84, 2	100	Terminase, large subunit
3F	1770–3242 (490)	<i>Lactobacillus</i> phage ilp84, 3	100	Portal
4F	3208–4200 (330)	<i>Lactobacillus</i> phage ilp84, 4	100	Scaffold
5F	4325–4963 (212)	<i>Lactobacillus</i> phage ilp84, 5	100	
6F	4976–5290 (104)	<i>Lactobacillus</i> phage ilp84, 6	100	
7F	5304–6344 (346)	<i>Lactobacillus</i> phage ilp84, 7	100	Major capsid
8F	6474–6851 (125)	<i>Lactobacillus</i> phage ilp84, 8	100	
9F	6855–7733 (292)	<i>Lactobacillus</i> phage ilp84, 9	100	
10F	7733–8107 (124)	<i>Lactobacillus</i> phage ilp84, 10	100	Head–tail joining
11F	8112–8414 (100)	<i>Lactobacillus</i> phage ilp84, 11	100	
12F	8411–8776 (121)	<i>Lactobacillus</i> phage ilp84, 12	100	Head–tail joining
13F	8777–9181 (134)	<i>Lactobacillus</i> phage ilp84, 13	100	
14F	9193–9792 (199)	<i>Lactobacillus</i> phage ilp84, 14	100	Major tail
15F	9931–10,266 (111)	<i>Lactobacillus</i> phage ilp84, 15	100	Tail assembly chaperone
16F	10,311–10,718 (135)	<i>Lactobacillus</i> phage ilp84, 16	100	Tail assembly chaperone
17F	10,711–14,046 (1112)	<i>Lactobacillus</i> phage ilp84, 17	100	Tape measure
18F	14,049–16,013 (654)	<i>Lactobacillus</i> phage ilp84, 18	100	Distal tail
19F	16,010–19,129 (1039)	<i>Lactobacillus</i> phage PL-1, 17	100	Tail associated lysozyme
20F	19,139–19,462 (107)	<i>Lactobacillus</i> phage A2, 15	100	
21F	19,567–19,917 (116)	<i>Lactobacillus</i> phage A2, 16	100	
22F	19,932–20,345 (137)	<i>Lactobacillus</i> phage ilp84, 22	99	Holin
23F	20,356–21,540 (394)	<i>Lactobacillus</i> phage ilp84, 23	100	Lysin
24F	21,585–21,809 (74)	<i>Lactobacillus</i> phage ilp84, 24	100	
25R	22,197–21,904 (97)	<i>Lactobacillus paracasei</i> subsp. <i>paracasei</i> lpp48	76 (QC 90)	
26R	23,403–22,219 (394)	<i>Lactobacillus</i> phage ilp84, 25	100	Integrase
27R	23,862–23,533 (109)	<i>Lactobacillus</i> phage ilp84, 26	100	
28R	24,313–23,855 (152)	<i>Lactobacillus</i> phage ilp84, 27	100	
29R	24,590–24,387 (67)	<i>Lactobacillus</i> phage ilp84, 28	100	
30R	25,039–24,614 (141)	<i>Lactobacillus</i> phage ilp84, 29	100	
31R	26,031–25,138 (297)	<i>Lactobacillus</i> phage ilp84, 30	100	
32R	27,437–26,082 (451)	<i>Clostridium</i> phage CDMH1	43 (QC81)	Replication
33R	27,865–27,515 (116)	<i>Lactobacillus</i> prophage Lj928 ( <i>Ljo_1464</i> )	49 (QC 75)	
34R	28,500–27,922 (192)	<i>Lactobacillus</i> phage ilp84, 31	29 (QC 47)	
35R	28,975–28,559 (138)	<i>Lactobacillus</i> phage ilp84, 32	93	
36R	29,306–28,968 (112)	<i>Lactobacillus</i> phage ilp84, 33	53	Transcriptional regulator
37F	29,446–29,646 (66)	<i>Listeria</i> phage vB_LmoS_293, 36	50 (QC 90)	Transcriptional regulator
38F	29,683–29,994 (103)	<i>Lactobacillus paracasei</i> subsp. <i>paracasei</i> lpp48 (04356)	98	
39R	30,209–29,991 (72)	<i>Lactobacillus paracasei</i> subsp. <i>paracasei</i> CNCM I-4649 ( <i>Lpp124_00315</i> )	100	
40F	30,288–30,434 (48)	<i>Lactobacillus</i> phage ilp84, 37	98	
41F	30,500–31,048 (182)	<i>Lactobacillus</i> phage ilp84, 38	98	
42F	31,027–31,248 (73)	<i>Lactobacillus</i> phage ilp84, 39	99	

**Table 2** (continued)

PLE2 gene strand	Start–stop (length-aa)	Best database match with virus (organism, gene)	% aa ident.	Predicted function
43F	31,261–31,389 (42)	<i>Lactobacillus</i> phage ilp84, 40	100	
44F	31,483–31,896 (137)	<i>Lactobacillus</i> phage ilp84, 42	99	
45F	31,909–32,772 (287)	<i>Lactobacillus</i> phage ilp84, 43	92	DNA binding
46F	32,852–33,553 (233)	<i>Lactobacillus</i> phage ilp84, 44	96	
47F	33,569–34,534 (321)	<i>Lactobacillus</i> phage ilp84, 45	95 (QC 57)	
48R	35,041–34,661 (126)	<i>Lactobacillus</i> phage ilp84, 47	100	
49F	35,376–35,588 (70)	<i>Lactobacillus</i> phage ilp84, 49	100	
50F	35,585–36,034 (149)	<i>Lactobacillus</i> phage ilp84, 50	100	
51F	36,081–36,335 (84)	<i>Lactobacillus</i> phage ilp84, 51	100	
52F	36,332–36,697 (121)	<i>Lactobacillus</i> phage ilp84, 52	100	Endodeoxyribonuclease
53F	36,710–37,003 (97)	<i>Lactobacillus</i> phage ilp84, 53	100	
54F	37,009–37,206 (65)	<i>Lactobacillus paracasei</i> subsp. <i>paracasei</i> Lpp125, <i>Lpp125_00822</i>	86	
55F	37,244–37,364 (46)	<i>Lactobacillus</i> phage ilp84, 55	96	
56F	37,577–38,020 (147)	<i>Lactobacillus</i> phage ilp84, 56	89	Transcriptional regulator
tRNA	38,484–38,559	<i>Lactobacillus</i> phage ilp84	97	tRNA-Ile
57F	38,616–38,996 (126)	<i>Lactobacillus</i> phage ilp84, 57	100 (QC 76)	
58F	39,090–39,281 (63)	<i>Lactobacillus</i> phage ilp84, 58	78	
59F	39,505–40,653 (382)	<i>Lactobacillus</i> phage ilp84, 59	89	
60F	40,646–40,969 (107)	<i>Lactobacillus</i> phage ilp84, 60	95	Ribonucleoside diphosphate reductase

Only values under 95 % are shown

QC query coverage

genes, 45 ORFs are transcribed rightwards, and 6 leftwards. PLE-3 presents 60 potential ORFs (46 rightwards and 14 leftwards) and encodes a tRNA<sup>Ile</sup>. Nucleotide sequence comparison with other LAB phages shows that PLE3 is most closely related to *Lactobacillus* phage iLp84 (query coverage 90 %, identity 99 %). Genome analysis of PLE2 revealed the presence

of a slippery sequence at the end of gene 11. Two tail proteins would be synthesized via a –1 programmed translational frameshift in gene 11 (CCAAAA), a major tail short protein (gp11), and a long protein (gp12) of 215 and 236 amino acids, respectively (Rodriguez et al. 2005; Seegers et al. 2004). A second frameshift, highly conserved in Siphoviridae that would lead to

**Fig. 3** Excision rate of PLEs. Using a real-time quantitative PCR assay, the ratio between the induction frequency (*attB*) for each PLE and the level of a chromosomal DNA gene (*prtP*) was calculated at the indicated time points after induction with mitomycin C (*M*) or in control cultures (*C*). Horizontal bars indicate mean ratios, and error bars represent the 95 % confidence intervals for the three separate replicate runs

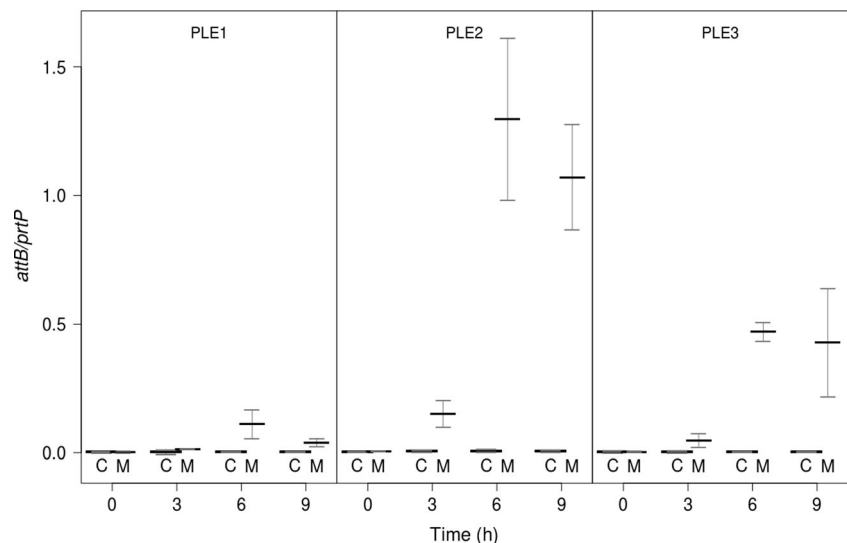
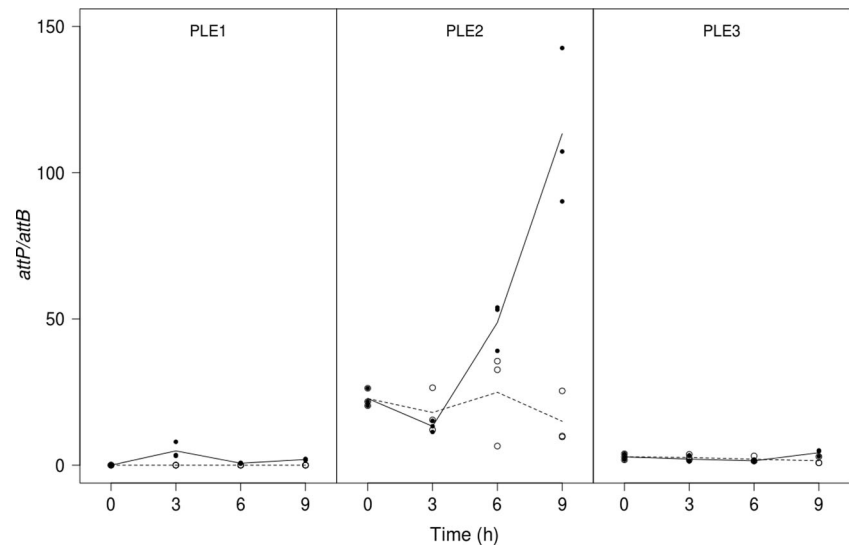




**Fig. 4** Replication of prophages after excision. Using a real-time quantitative PCR assay, the ratio between the circularized form of the prophage (*attP*) and *attB* was calculated at the indicated time points after induction with mitomycin C (closed circles) or in control cultures (open circles) for each separate replicate run



the production of two tail assembly chaperones (Xu et al. 2004), was found in PLE2. A slippery sequence (AAAAAAATA) is found at the end of gene 13 that could facilitate expression of the longer form (gp14). It is noteworthy that this conserved frameshift in the assembly chaperones genes is absent in PLE3 genome. In PLE3, two chaperones could be present but encoded by two different genes, 15 and 16, separated by a short intergenic region.

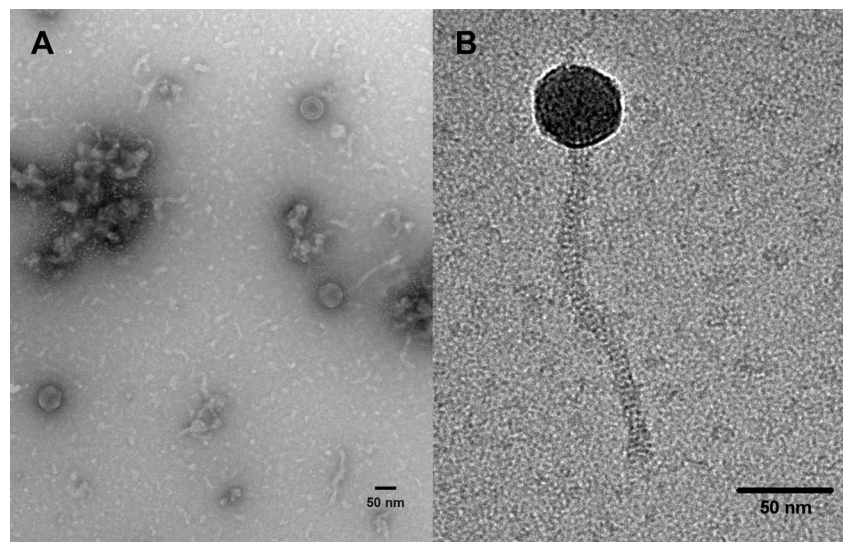
Both phages carry integrases of the tyrosine family in their genomes (gene 24 for PLE2; gene 26 for PLE3). HHpred analysis shows high similarity with lambda integrase (pdb:1z1b, probability = 100 %, identity 17 % for PLE2 and probability = 100 %, identity 25 % for PLE3). In the C-terminal region (catalytic domain), the putative catalytic

tyrosine is located at positions 361 and 373 for PLE2 and PLE3, respectively, and the possible RKHRH pentad was also found in this region. The *attP* site for PLE2 is positioned at 19,589–19,658 in an intergenic region between the lysin (gene 23) and the integrase (gene 24). Interestingly for PLE3, the putative *attP* site is located between 22,006 and 22,103 of gene 25 that is disrupted in the integrated form.

As shown in Table 3, MS analysis of the protein bands from the SDS-PAGE of CsCl purified partial lysates revealed that most of the identified proteins corresponded to PLE2 and only two proteins (including the capsid protein) corresponded to PLE3.

Striking differences were found in the baseplate proteins of both phages that are presented in detail below.

**Fig. 5** Electron microscopy of induced prophages. Supernatants from partially lysed cultures of *L. casei* BL23 after 9 h of induction with mitomycin C were collected and concentrated by ultracentrifugation for inspection by electron microscopy. **a** Phage heads and disassociated tails are mainly observed. **b** Representative image of the induced prophage



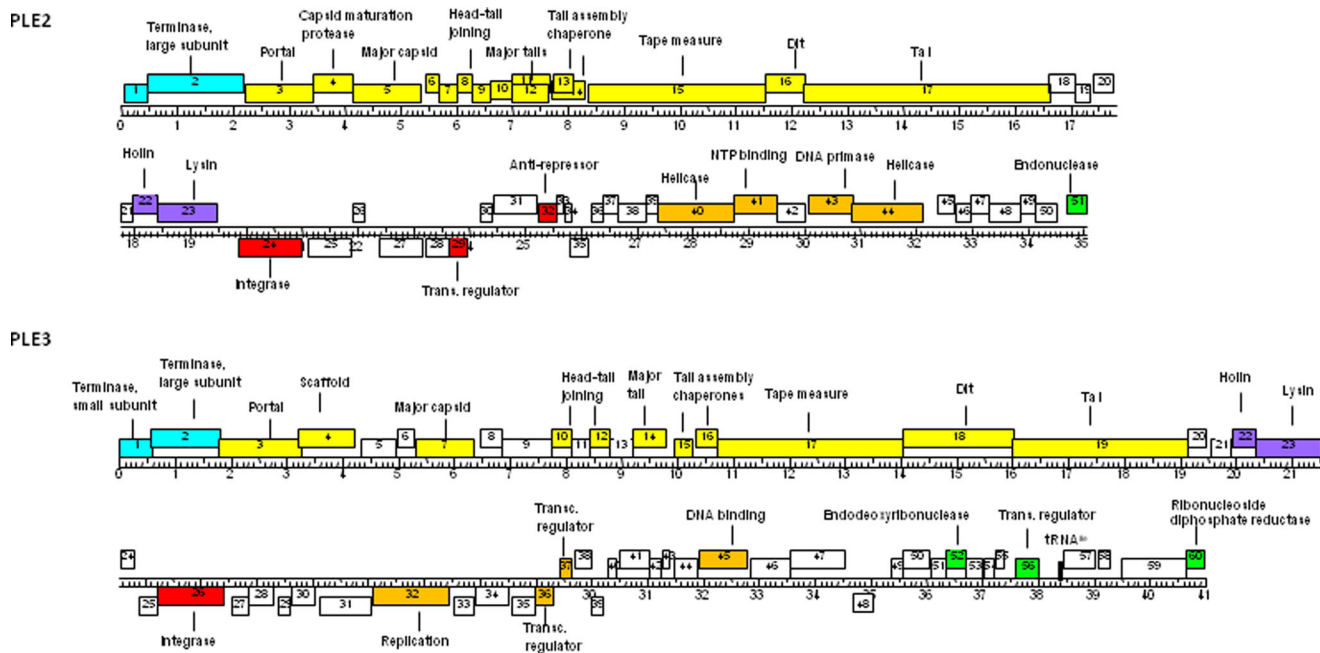


**Fig. 6** Annotated genome maps of PLE2 and PLE3. The viral genomes of PLE2 and PLE3 are represented in four tiers with markers spaced at 1-kbp and 100-bp intervals. The predicted genes are shown as boxes either above or below the genome, depending on whether they are rightwards or leftwards transcribed, respectively. Gene numbers are shown within each

box. Putative genes can be divided in the following six modules: packaging (light blue), virion structure (yellow), lysis (purple), integration and immunity (red), and replication (orange). The putative proteins found in the extreme right region are colored in green, while the ORFs lacking function are white colored

### Comparison of baseplate proteins among *Lactobacillus* phages and prophages

A previous analysis of baseplate proteins of *L. casei* phages J-1 and PL-1, as compared with other *Lactobacillus* phages, revealed that the overall canonical organization of the Dlt and Tal proteins seemed to be conserved (Dieterle et al. 2014a), although with some remarkable differences with the related proteins from lactococcal phages (Veesler and Cambillau 2011). In all the analyzed phages (including phiAT3, Lrm1,

Lc-Nu, and A2), two high molecular mass Dlt and Tal proteins were identified, but no baseplate/tip peripheral proteins (such as canonical RBPs) could be detected.

HHpred (Soding et al. 2005) analysis revealed that the N-terminal segment of Dlt (the belt ring) is conserved, but two putative distinctive CBMs were identified in the C-terminal segment of the protein that presumably could interact with bacterial saccharide receptors. For the Tal proteins, the N-terminus (residues 1 to ~370) has the canonical structure similar to that of phage T4 gp27 and to most other Siphoviridae (Veesler and Cambillau 2011). It further projects out a long C-terminus that might be involved in bacterial recognition or cell wall degradation.

Comparison of baseplate proteins of PLE1, PLE2, and PLE3 and other prophages induced from strains of the *L. casei* group showed similarities but also remarkable differences with this pattern (Supplementary Fig. S1).

Dlt proteins of PLE1, PLE2 (orf 16), and iA2 are 231 residues long, are almost identical, and belong to the classical Dlt type illustrated in the structures from phages SPP1 (Veesler et al. 2010) and TP901-1 (Bebeacua et al. 2010; Veesler et al. 2012) (Supplementary Fig. S1A and Fig. 7a). This molecule is assembled as a hexamer forming a ring with a 40-Å internal diameter and projecting a galectin-like domain at the periphery. Worth noticing, phage's T5 Dlt is decorated by an OB-fold domain, instead of a galectin-like one (Flayhan

**Table 3** Identification of virion-associated proteins

gp	MW [kDa]	Coverage <sup>a</sup>	PSMs
PLE2			
gp3 (portal)	45.7	0.59	161
gp5 (major capsid)	43.7	0.22	15
gp9 (head–tail joining?)	12.5	0.22	5
gp11/12 (major tails)	15.9	0.24	14
gp15 (TMP)	112.4	0.03	7
PLE3			
gp6 (head–tail joining?)	10.7	0.40	2
gp7 (major capsid)	38.2	0.36	15

PSMs peptide spectrum matches

<sup>a</sup> Percentage of predicted protein sequence identified in peptides

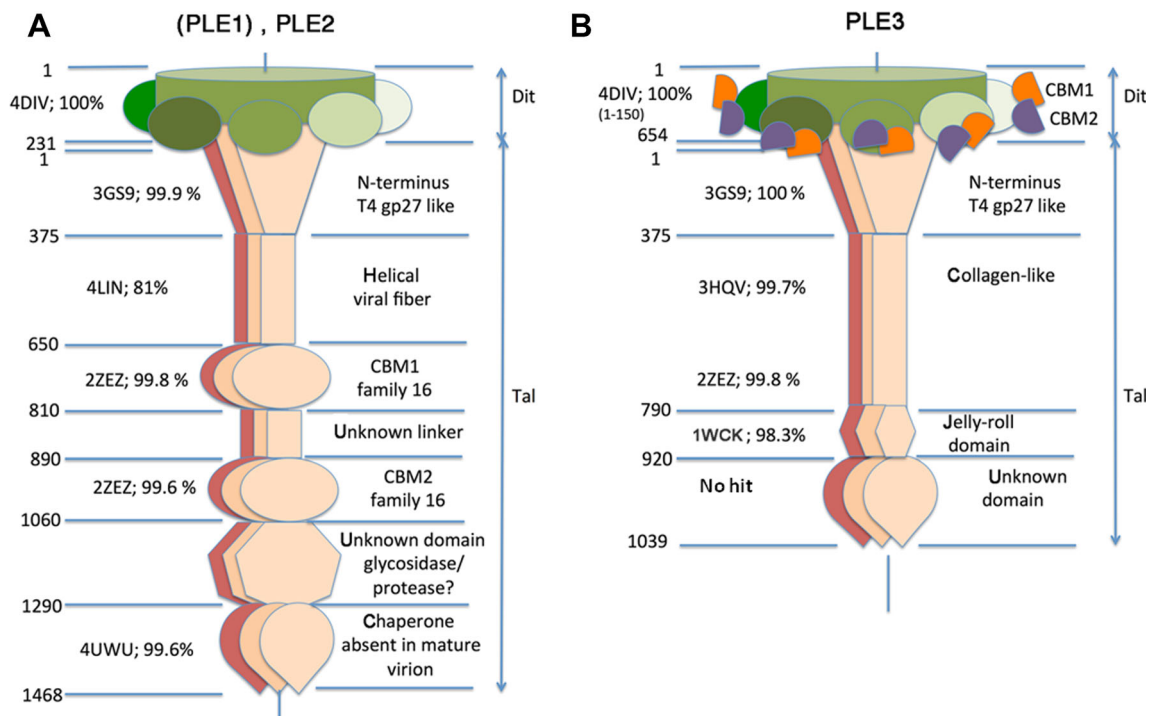


**Fig. 7** Schematic representation of baseplate proteins of PLE1/PLE2 and PLE3 based on HHpred analysis. **a** Baseplate of phages PLE1 and PLE2. **b** Baseplate of phage PLE3. The HHpred retrieved PDB template is indicated as well as the similarity probability (in %) returned by

HHpred. Hexameric classical Dits are depicted as a *flat green cylinder* for the belt domains and *green circles* for the galectin domains. PLE3 evolved Dit CBM1 and CBM2 are colored in *orange* and *violet*, respectively. Trimeric Tal proteins are colored *beige/brown*

et al. 2014). In contrast, PLE3 Dit (orf 18) exhibits two insertions, one just after the N-terminus of the belt domain and the second within the first loop of the galectin-like domain, a feature observed in, e.g., phages J-1 and PL-1 Dits (Supplementary Fig. S1C and Fig. 7b). By analogy with the type VI secretion system VgrG protein (Pukatzki et al. 2007), we call this insertion-containing Dit “evolved” Dit. While in the case of phages J-1 the first insertion could be assigned unambiguously by HHpred (Soding et al. 2005) to a carbohydrate binding domain (CBM), HHpred did not retrieve any significant hit in the PDB for the first insertion of the PLE3 Dit. However, sequence alignment of PLE3 and J-1 Dits (Supplementary Fig. S1C) revealed that their putative first CBM (CBM1) domains are similar, suggesting that PLE3 CBM1 may also be a bona fide CBM domain (Fig. 7b). Worth noticing, the two PLE3 Dit inserted CBMs share 32 % similarity and 25 % identity (Supplementary Fig. S1D), signature of a common overall fold. Furthermore, Dits from iLp1308 (from *L. paracasei* CNRZ 1308), CL1, CL2 (from *L. paracasei* A), and iLp84 (from *L. paracasei* 84) also contain two insertions (Supplementary Fig. S2). Their first insertion is also predicted as a CBM domain by HHpred with probabilities better than 95 %. Concerning the J-1/PLE3 second insertion, also found in the abovementioned phages, HHpred did not report any hit. However, we recently determined the structure of the second insertion domain of

phage J-1, which revealed to be a true CBM domain (Dieterle et al., paper in preparation). Hence, due to sequence similarity, the second insertions in the Dits of the phages under scrutiny here can be defined as a second CBM (CBM2) (Fig. 7b). Remarkably, the putative CBM2 is indistinguishable in all the above-analyzed proteins.

All Tal proteins analyzed here have the first ~370 amino acids with the predicted classical fold of gp27 (Kanamaru et al. 2002; Kondou et al. 2005) and phage p2 ORF16 (Sciara et al. 2010). Again, Tal proteins from CL1, CL2, and iLp1308 are identical and slightly different from those from PLE3 and iLp84, these two latter Tal proteins being identical. HHpred analysis was not able to detect any documented structure for the C-terminus of these proteins, although a number of putative collagen repeats were detected in the middle segment of these Tals, a feature also found for J-1 and PL-1 phages Tals.

PLE1 (iA2) and PLE2 (orf 17) Tals exhibit also a classical N-terminal domain (residues 1–374) (Supplementary Fig. S1B and Fig. 7a). After this segment, a fibrin-like tail needle domain (residues 375–649) is identified by HHpred (Fig. 7a). This domain, probably extended, links the N-terminus to a HHpred predicted carbohydrate binding domain (650–817) (Fig. 7a), followed by a short undetermined segment (818–880) and a glycosidase or CBM domain (881–1060). The next undetermined segment (1061–1292) (Fig. 7a) is followed by a domain that was assigned by

HHpred to a chaperone, the PDB target being the L-shaped tail-fiber chaperone that helps folding of a glycosidase (1293–1468) (Fig. 7a) (Garcia-Doval et al. 2015). However, this chaperone is very far in sequence from the glycosidase/CBM identified at residues 881–1060. This may signify that the structurally unknown 1293–1468 segment might be a protease/glycosidase with a structure not documented in the PDB. Worth noticing, the sequences of PLE1/iA2 and PLE2 Tals are 99 % identical (Supplementary Fig. S1B) except for the segment before the chaperone (residues 1170–1350), covering essentially the unknown segment that might be assigned to a protease/glycosidase. This feature may correlate to differences in host cell wall hydrolysis between PLE1 and PLE2.

PLE3 Tal (orf 19), as in the other analyzed prophages, is composed of the classical N-terminal domain (1–390) followed by a long collagen-like structure (450–930) and a C-terminal segment of unknown structure (931–1040) (Fig. 7b).

## Discussion

*L. casei* BL23 is a widely used laboratory strain that was obtained when trying to cure *L. casei* ATCC 393 of a plasmid (Acedo-Felix and Perez-Martinez 2003). Although it has been demonstrated that *L. casei* ATCC 393 was not the ancestral of BL23 (Diancourt et al. 2007), it has been extensively used for physiological, biochemical, and genetic studies (Bourand et al. 2013; Munoz-Provencio et al. 2012; Piuri et al. 2003; Revilla-Guarinos et al. 2013) and it has been shown that it exhibits probiotic properties (Rochat et al. 2007). Despite of its extensive use, the presence of a mobile element in *L. casei* BL23 has only been briefly described during the release of the complete bacterial genome sequence (Maze et al. 2010) and recently while analyzing by bioinformatics the presence of prophages in different *Lactobacillus* strains (Mercanti et al. 2015). Prophage stability should be considered when using this strain for different studies since, as it has been shown in other systems, the presence of prophages (Ojha et al. 2005) or its excision can influence the bacterial phenotype (Rabinovich et al. 2012).

In this work, we described the presence of three complete prophages (PLE1–3) in the genome of *L. casei* BL23. Interestingly, one of these prophages, PLE1, is 99 % similar to the recently sequenced iA2 phage isolated after induction of the probiotic *L. paracasei* A strain (Capra et al. 2010), but unlike iA2, we were not able to induce it after mitomycin C exposure. PLE1 has a small deletion of 5 bp in the integration/immunity region that could account for this different behavior. Under our conditions, we were able to induce two other prophages, PLE2 and PLE3, even though at different rates. Based on the position in the genome, PLE2 is identified as the reported mobilized prophage found during sequencing of the *L. casei* BL23 strain (Maze et al. 2010). Using a quantitative

real-time PCR approach, we demonstrated that the rate of excision was higher for PLE2 than for PLE3 and the circularized phage genome of PLE2 further replicates suggesting that complete phage particles are assembled. This result correlated with an overrepresented proportion of PLE2, in comparison to PLE3, observed during DNA sequencing of phage from partial lysates. Moreover, MS analysis of phage proteins from the same lysates showed that the majority of proteins corresponded to PLE2 while only the more abundant proteins (e.g., capsid protein) of PLE3 were present. Neither by sequencing nor MS protein analysis could PLE1 be detected and the ratio *attB/prtP* merely increased for this prophage after MC induction.

High rates of spontaneous induction of prophages and their ability to acquire bacterial genes and transduce them to related strains were described in *Lactobacillus gasseri* ADH suggesting that temperate bacteriophages likely contribute to horizontal gene transfer (HGT) (Baugher et al. 2014; Raya and Klaenhammer 1992). Even though our data shows a low level of spontaneous induction in the condition tested, the multiple prophages found in *L. casei* BL23, their sequence similarities, and also high homologies found with other phages or prophages present in other *Lactobacillus* strains contribute to the idea of HGT and high rates of recombination events.

All phages analyzed here do not harbor baseplate peripheral proteins, such as RBPs, involved in host cell wall saccharide binding. Phage PLE3, however, shares some characteristics with phages J-1 and PL-1, as all possess evolved Dit proteins. The insertion of CBMs in these evolved Dit suggests that they might replace bona fide RBPs for cell wall saccharide binding. Interestingly, while the Dits from PLE1 and PLE2 phages are not evolved, their Tal proteins harbor at least two different CBMs that might be involved in cell wall saccharide binding. Phage iA2/PLE1 and PLE2 Tal proteins display significant structural differences compared to other analyzed *L. casei* phages. Our results provide first evidences of Dit/Tal-inserted modules that may replace RBPs in host cell wall binding, a feature that may extend to many other phages from diverse origins.

The increasing use of strains of *L. casei* in commercial preparations has led to a clear interest in bacteriophages that can infect *Lactobacillus* spp. Induced temperate phages not only can lyse the starter strains (Mercanti et al. 2011) but also can give rise to new lytic phages that can infect and lyse sensitive strains in a mixed culture use for dairy fermentations (Moineau et al. 1995). Different factors present during fermentation processes such as osmolarity, pH, and temperature fluctuations could act as prophage inducers and need to be tested in the future to avoid host lysis that would lead to fermentation failures not only in starter strains but also in potential probiotic strains. Adsorption is a key step for phage propagation, and inhibition of this process can advantageously be used to prevent infection.

**Acknowledgments** We thank Raul Raya from CERELA for testing of induced prophages in different *Lactobacillus* spp. strains.

### Compliance with ethical standards

**Funding** This work was partially supported by UBACYT 2014-2017 GC 20020130100444BA to MP. M.E.D. is a doctoral fellow of Consejo Nacional de Investigaciones Científicas y Tecnológicas (CONICET, Argentina).

**Conflict of interest** All authors declare that they have no conflict of interest.

**Ethical approval** This article does not contain any studies with human participants or animals performed by any of the authors.

## References

- Acedo-Felix E, Perez-Martinez G (2003) Significant differences between *Lactobacillus casei* subsp. *casei* ATCC 393T and a commonly used plasmid-cured derivative revealed by a polyphasic study. *Int J Syst Evol Microbiol* 53:67–75. doi:10.1099/ijs.0.02325-0
- Ai L, Chen C, Zhou F, Wang L, Zhang H, Chen W, Guo B (2011) Complete genome sequence of the probiotic strain *Lactobacillus casei* BD-II. *J Bacteriol* 193:3160–3161. doi:10.1128/jb.00421-11
- Altschul SF, Gish W, Miller W, Myers EW, Lipman DJ (1990) Basic local alignment search tool. *J Mol Biol* 215:403–410. doi:10.1016/s0022-2836(05)80360-2
- Baugher JL, Durmaz E, Klaenhammer TR (2014) Spontaneously induced prophages in *Lactobacillus gasseri* contribute to horizontal gene transfer. *Appl Environ Microbiol* 80:3508–3517. doi:10.1128/aem.04092-13
- Bebeacua C, Bron P, Lai L, Vegge CS, Brondsted L, Spinelli S, Campanacci V, Veessler D, van Heel M, Cambillau C (2010) Structure and molecular assignment of lactococcal phage TP901-1 baseplate. *J Biol Chem* 285:39079–39086. doi:10.1074/jbc.M110.175646
- Borodovsky M, McIninch J (1993) Recognition of genes in DNA sequence with ambiguities. *Biosystems* 30:161–171
- Bourand A, Yebra MJ, Boel G, Maze A, Deutscher J (2013) Utilization of D-ribitol by *Lactobacillus casei* BL23 requires a mannose-type phosphotransferase system and three catabolic enzymes. *J Bacteriol* 195:2652–2661. doi:10.1128/jb.02276-12
- Canchaya C, Proux C, Fournous G, Bruttin A, Brussow H (2003) Prophage genomics. *Microbiol Mol Biol Rev* 67:238–276
- Capra ML, Mercanti DJ, Reinheimer JA, Quiberoni AL (2010) Characterisation of three temperate phages released from the same *Lactobacillus paracasei* commercial strain. *Int J Dairy Technol* 63:396–405. doi:10.1111/j.1471-0307.2010.00600.x
- Chen C, Ai L, Zhou F, Wang L, Zhang H, Chen W, Guo B (2011) Complete genome sequence of the probiotic bacterium *Lactobacillus casei* LC2W. *J Bacteriol* 193:3419–3420. doi:10.1128/jb.05017-11
- Delcher AL, Harmon D, Kasif S, White O, Salzberg SL (1999) Improved microbial gene identification with GLIMMER. *Nucleic Acids Res* 27:4636–4641
- Diancourt L, Passet V, Chervaux C, Garault P, Smokvina T, Brisse S (2007) Multilocus sequence typing of *Lactobacillus casei* reveals a clonal population structure with low levels of homologous recombination. *Appl Environ Microbiol* 73:6601–6611. doi:10.1128/aem.01095-07
- Dieterle ME, Bowman C, Batthyany C, Lanzarotti E, Turjanski A, Hatfull G, Piuri M (2014a) Exposing the secrets of two well-known *Lactobacillus casei* phages, J-1 and PL-1, by genomic and structural analysis. *Appl Environ Microbiol* 80:7107–7121. doi:10.1128/AEM.02771-14
- Dieterle ME, Jacobs-Sera D, Russell D, Hatfull G, Piuri M (2014b) Complete genome sequences of *Lactobacillus* phages J-1 and PL-1. *Genome Announc*. doi:10.1128/genomeA.00998-13
- Douillard FP, Kant R, Ritari J, Paulin L, Palva A, de Vos WM (2013a) Comparative genome analysis of *Lactobacillus casei* strains isolated from Actimel and Yakult products reveals marked similarities and points to a common origin. *Microb Biotechnol* 6:576–587. doi:10.1111/1751-7915.12062
- Douillard FP, Ribbera A, Jarvinen HM, Kant R, Pietila TE, Randazzo C, Paulin L, Laine PK, Caggia C, von Ossowski I, Reunanen J, Satokari R, Salminen S, Palva A, de Vos WM (2013b) Comparative genomic and functional analysis of *Lactobacillus casei* and *Lactobacillus rhamnosus* strains marketed as probiotics. *Appl Environ Microbiol* 79:1923–1933. doi:10.1128/AEM.03467-12
- Douillard FP, Ribbera A, Kant R, Pietila TE, Jarvinen HM, Messing M, Randazzo CL, Paulin L, Laine P, Ritari J, Caggia C, Lahtinen T, Brouns SJ, Satokari R, von Ossowski I, Reunanen J, Palva A, de Vos WM (2013c) Comparative genomic and functional analysis of 100 *Lactobacillus rhamnosus* strains and their comparison with strain GG. *PLoS Genet* 9:e1003683. doi:10.1371/journal.pgen.1003683
- Durmaz E, Klaenhammer TR (2000) Genetic analysis of chromosomal regions of *Lactococcus lactis* acquired by recombinant lytic phages. *Appl Environ Microbiol* 66:895–903
- Durmaz E, Miller MJ, Azcarate-Peril MA, Toon SP, Klaenhammer TR (2008) Genome sequence and characteristics of Lm1, a prophage from industrial *Lactobacillus rhamnosus* strain M1. *Appl Environ Microbiol* 74:4601–4609. doi:10.1128/AEM.00010-08
- Echols H (1972) Developmental pathways for the temperate phage: lysis vs lysogeny. *Annu Rev Genet* 6:157–190. doi:10.1146/annurev.ge.06.120172.001105
- Flayhan A, Vellieux FM, Lurz R, Maury O, Contreras-Martel C, Girard E, Boulanger P, Breyton C (2014) Crystal structure of pb9, the distal tail protein of bacteriophage T5: a conserved structural motif among all siphophages. *J Virol* 88:820–828. doi:10.1128/JVI.02135-13
- Garcia P, Ladero V, Suarez JE (2003) Analysis of the morphogenetic cluster and genome of the temperate *Lactobacillus casei* bacteriophage A2. *Arch Virol* 148:1051–1070. doi:10.1007/s00705-003-0008-x
- Garcia-Doval C, Caston JR, Luque D, Granell M, Otero JM, Llamas-Saiz AL, Renouard M, Boulanger P, van Raaij MJ (2015) Structure of the receptor-binding carboxy-terminal domain of the bacteriophage T5 L-shaped tail fibre with and without its intra-molecular chaperone. *Viruses* 7:6424–6440. doi:10.3390/v7122946
- Gameau JE, Moineau S (2011) Bacteriophages of lactic acid bacteria and their impact on milk fermentations. *Microb Cell Fact* 10 Suppl 1: S20. doi:10.1186/1475-2859-10-S1-S20
- Gordon D (2003) Viewing and editing assembled sequences using Consed. *Curr Protoc Bioinformatics Chapter 11:Unit11.12*. doi:10.1002/0471250953.bi1102s02
- Hino MIN (1965) Lactic acid bacteria employed for beverage production. II. Isolation and some properties of a bacteriophage isolated during the fermentation of lactic acid beverage. *J Chem Soc Japan* 39:472–476
- Hochwind K, Weinmaier T, Schmid M, van Hemert S, Hartmann A, Rattei T, Rothballer M (2012) Draft genome sequence of *Lactobacillus casei* W56. *J Bacteriol* 194:6638. doi:10.1128/jb.01386-12
- Kanamaru S, Leiman PG, Kostyuchenko VA, Chipman PR, Mesyanzhinov VV, Arisaka F, Rossmann MG (2002) Structure of the cell-puncturing device of bacteriophage T4. *Nature* 415:553–557. doi:10.1038/415553a

- Kondou Y, Kitazawa D, Takeda S, Tsuchiya Y, Yamashita E, Mizuguchi M, Kawano K, Tsukihara T (2005) Structure of the central hub of bacteriophage Mu baseplate determined by X-ray crystallography of gp44. *J Mol Biol* 352:976–985. doi:10.1016/j.jmb.2005.07.044
- Laslett D, Canbäck B (2004) ARAGORN, a program to detect tRNA genes and tmRNA genes in nucleotide sequences. *Nucleic Acids Res* 32:11–16. doi:10.1093/nar/gkh152
- Lo TC, Shih TC, Lin CF, Chen HW, Lin TH (2005) Complete genomic sequence of the temperate bacteriophage PhiAT3 isolated from *Lactobacillus casei* ATCC 393. *Virology* 339:42–55. doi:10.1016/j.virol.2005.05.022
- Lowe TM, Eddy SR (1997) tRNAscan-SE: a program for improved detection of transfer RNA genes in genomic sequence. *Nucleic Acids Res* 25:955–964
- Lunde M, Blatny JM, Kaper F, Nes IF, Lillehaug D (2000) The life cycles of the temperate lactococcal bacteriophage phiLC3 monitored by a quantitative PCR method. *FEMS Microbiol Lett* 192:119–124
- Lunde M, Blatny JM, Lillehaug D, Aastveit AH, Nes IF (2003) Use of real-time quantitative PCR for the analysis of LC3 prophage stability in Lactococci. *App Environ Microbiol* 69:41–48. doi:10.1128/aem.69.1.41-48.2003
- Maldonado Galdeano C, Novotny Nunez I, Carmuega E, de Moreno de LeBlanc A, Perdigon G (2015) Role of probiotics and functional foods in health: gut immune stimulation by two probiotic strains and a potential probiotic yoghurt. *Endocr Metab Immune Disord Drug Targets* 15:37–45
- Marchler-Bauer A, Bryant SH (2004) CD-Search: protein domain annotations on the fly. *Nucleic Acids Res* 32:W327–W331. doi:10.1093/nar/gkh454
- Maze A, Boel G, Zuniga M, Bourand A, Loux V, Yebra MJ, Monedero V, Correia K, Jacques N, Beauflis S, Poncet S, Joyet P, Milohanic E, Casaregola S, Auffray Y, Perez-Martinez G, Gibrat JF, Zagorec M, Francke C, Hartke A, Deutscher J (2010) Complete genome sequence of the probiotic *Lactobacillus casei* strain BL23. *J Bacteriol* 192:2647–2648. doi:10.1128/jb.00076-10
- McFarland LV (2015) From yaks to yogurt: the history, development, and current use of probiotics. *Clin Infect Dis* 60(Suppl 2):S85–S90. doi:10.1093/cid/civ054
- Mercanti DJ, Carminati D, Reinheimer JA, Quiberoni A (2011) Widely distributed lysogeny in probiotic lactobacilli represents a potentially high risk for the fermentative dairy industry. *Int J Food Microbiol* 144:503–510. doi:10.1016/j.ijfoodmicro.2010.11.009
- Mercanti DJ, Rousseau GM, Capra ML, Quiberoni A, Tremblay DM, Labrie SJ, Moineau S (2015) Genomic diversity of phages infecting probiotic strains of *Lactobacillus paracasei*. *Appl Environ Microbiol* 82:95–105. doi:10.1128/aem.02723-15
- Moineau S, Pandian S, Klaenhammer TR (1995) Specific chromosomal sequences can contribute to the appearance of a new lytic bacteriophage in *Lactococcus*. *Dev Biol Stand* 85:577–580
- Munoz-Provencio D, Rodriguez-Diaz J, Collado MC, Langella P, Bermudez-Humaran LG, Monedero V (2012) Functional analysis of the *Lactobacillus casei* BL23 sortases. *Appl Environ Microbiol* 78:8684–8693. doi:10.1128/aem.02287-12
- Ojha A, Anand M, Bhatt A, Kremer L, Jacobs WR Jr, Hatfull GF (2005) GroEL1: a dedicated chaperone involved in mycolic acid biosynthesis during biofilm formation in mycobacteria. *Cell* 123:861–873. doi:10.1016/j.cell.2005.09.012
- Piuri M, Sanchez-Rivas C, Ruzal SM (2003) Adaptation to high salt in *Lactobacillus*: role of peptides and proteolytic enzymes. *J Appl Microbiol* 95:372–379
- Pukatzki S, Ma AT, Revel AT, Sturtevant D, Mekalanos JJ (2007) Type VI secretion system translocates a phage tail spike-like protein into target cells where it cross-links actin. *Proc Natl Acad Sci U S A* 104:15508–15513. doi:10.1073/pnas.0706532104
- Rabinovich L, Sigal N, Borovok I, Nir-Paz R, Herskovits AA (2012) Prophage excision activates *Listeria* competence genes that promote phagosomal escape and virulence. *Cell* 150:792–802. doi:10.1016/j.cell.2012.06.036
- Raya RR, H'Bert EM (2009) Isolation of phage via induction of lysogens. *Methods Mol Biol* 501:23–32. doi:10.1007/978-1-60327-164-6\_3
- Raya RR, Klaenhammer TR (1992) High-frequency plasmid transduction by *Lactobacillus gasserii* bacteriophage phiadh. *Appl Environ Microbiol* 58:187–193
- Revilla-Guarinos A, Gebhard S, Alcantara C, Staron A, Mascher T, Zuniga M (2013) Characterization of a regulatory network of peptide antibiotic detoxification modules in *Lactobacillus casei* BL23. *Appl Environ Microbiol* 79:3160–3170. doi:10.1128/aem.00178-13
- Rochat T, Bermudez-Humaran L, Gratadoux JJ, Fourage C, Hoebler C, Corthier G, Langella P (2007) Anti-inflammatory effects of *Lactobacillus casei* BL23 producing or not a manganese-dependant catalase on DSS-induced colitis in mice. *Microb Cell Fact* 6:22. doi:10.1186/1475-2859-6-22
- Rodriguez I, Garcia P, Suarez JE (2005) A second case of -1 ribosomal frameshifting affecting a major virion protein of the *Lactobacillus* bacteriophage A2. *J Bacteriol* 187:8201–8204. doi:10.1128/JB.187.23.8201-8204.2005
- Ruggirello M, Dolci P, Cocolin L (2014) Detection and viability of *Lactococcus lactis* throughout cheese ripening. *PLoS One* 9:e114280. doi:10.1371/journal.pone.0114280
- Sciara G, Bebeacua C, Bron P, Tremblay D, Ortiz-Lombardia M, Lichiere J, van Heel M, Campanacci V, Moineau S, Cambillau C (2010) Structure of lactococcal phage p2 baseplate and its mechanism of activation. *Proc Natl Acad Sci U S A* 107:6852–6857. doi:10.1073/pnas.1000232107
- Seegers JF, Mc Grath S, O'Connell-Motherway M, Arendt EK, van de Guchte M, Creaven M, Fitzgerald GF, van Sinderen D (2004) Molecular and transcriptional analysis of the temperate lactococcal bacteriophage Tuc 2009. *Virology* 329:40–52. doi:10.1016/j.virol.2004.07.003
- Smid EJ, Erku O, Spus M, Wolkers-Rooijackers JC, Alexeeva S, Kleerebezem M (2014) Functional implications of the microbial community structure of undefined mesophilic starter cultures. *Microb Cell Fact* 13 Suppl 1:S2. doi:10.1186/1475-2859-13-s1-s2
- Soding J, Biegert A, Lupas AN (2005) The HHpred interactive server for protein homology detection and structure prediction. *Nucleic Acids Res* 33:W244–W248. doi:10.1093/nar/gki408
- Stein LD, Mungall C, Shu S, Caudy M, Mangone M, Day A, Nickerson E, Stajich JE, Harris TW, Arva A, Lewis S (2002) The generic genome browser: a building block for a model organism system database. *Genome Res* 12:1599–1610. doi:10.1101/gr.403602
- Tuohimaa A, Riipinen KA, Brandt K, Alatossava T (2006) The genome of the virulent phage Le-Nu of probiotic *Lactobacillus rhamnosus*, and comparative genomics with *Lactobacillus casei* phages. *Arch Virol* 151:947–965. doi:10.1007/s00705-005-0672-0
- Veesler D, Cambillau C (2011) A common evolutionary origin for tailed-bacteriophage functional modules and bacterial machineries. *Microbiol Mol Biol Rev* 75:423–433, first page of table of contents. doi:10.1128/MMBR.00014-11
- Veesler D, Robin G, Lichiere J, Auzat I, Tavares P, Bron P, Campanacci V, Cambillau C (2010) Crystal structure of bacteriophage SPP1 distal tail protein (gp19.1): a baseplate hub paradigm in gram-positive infecting phages. *J Biol Chem* 285:36666–36673. doi:10.1074/jbc.M110.157529
- Veesler D, Spinelli S, Mahony J, Lichiere J, Blangy S, Bricogne G, Legrand P, Ortiz-Lombardia M, Campanacci V, van Sinderen D, Cambillau C (2012) Structure of the phage TP901-1 1.8 MDa baseplate suggests an alternative host adhesion mechanism. *Proc Natl Acad Sci U S A* 109:8954–8958. doi:10.1073/pnas.1200966109
- Ventura M, Chanchaya C, Bernini V, Altermann E, Barrangou R, McGrath S, Claesson MJ, Li Y, Leahy S, Walker CD, Zink R, Neviani E, Steele J, Broadbent J, Klaenhammer TR, Fitzgerald GF, O'Toole PW, van Sinderen D (2006) Comparative genomics and

- transcriptional analysis of prophages identified in the genomes of *Lactobacillus gasseri*, *Lactobacillus salivarius*, and *Lactobacillus casei*. *Appl Environ Microbiol* 72:3130–3146. doi:[10.1128/AEM.72.5.3130-3146.2006](https://doi.org/10.1128/AEM.72.5.3130-3146.2006)
- Verreault D, Moineau S, Duchaine C (2008) Methods for sampling of airborne viruses. *Microbiol Mol Biol Rev* 72:413–444. doi:[10.1128/membr.00002-08](https://doi.org/10.1128/membr.00002-08)
- Villion M, Moineau S (2009) Bacteriophages of *Lactobacillus*. *Front Biosci* 14:1661–1683
- Watanabe K, Takesue S, Jin-Nai K, Yoshikawa T (1970) Bacteriophage active against the lactic acid beverage-producing bacterium *Lactobacillus casei*. *Appl Microbiol* 20:409–415
- Xu J, Hendrix RW, Duda RL (2004) Conserved translational frameshift in dsDNA bacteriophage tail assembly genes. *Mol Cell* 16:11–21. doi:[10.1016/j.molcel.2004.09.006](https://doi.org/10.1016/j.molcel.2004.09.006)
- Zhou Y, Liang Y, Lynch KH, Dennis JJ, Wishart DS (2011) PHAST: a fast phage search tool. *Nucleic Acids Res* 39:W347–W352. doi:[10.1093/nar/gkr485](https://doi.org/10.1093/nar/gkr485)